

Determination of limit cycles using stroboscopic set-valued maps

Jawher Jerray, Laurent Fribourg

► To cite this version:

Jawher Jerray, Laurent Fribourg. Determination of limit cycles using stroboscopic set-valued maps. ADHS 2021 - 7th IFAC Conference on Analysis and Design of Hybrid Systems, Jul 2021, Brussels, Belgium. hal-03249763

HAL Id: hal-03249763

<https://hal.archives-ouvertes.fr/hal-03249763>

Submitted on 4 Jun 2021

HAL is a multi-disciplinary open access archive for the deposit and dissemination of scientific research documents, whether they are published or not. The documents may come from teaching and research institutions in France or abroad, or from public or private research centers.

L'archive ouverte pluridisciplinaire **HAL**, est destinée au dépôt et à la diffusion de documents scientifiques de niveau recherche, publiés ou non, émanant des établissements d'enseignement et de recherche français ou étrangers, des laboratoires publics ou privés.

Determination of limit cycles using stroboscopic set-valued maps

Jawher Jerry* Laurent Fribourg**

* Université Sorbonne Paris Nord, LIPN, CNRS, Villetaneuse, France

** Université Paris-Saclay, CNRS, ENS Paris-Saclay, LMF, F91190 Gif-sur-Yvette, France

Abstract

Given a dynamical system Σ_p with a parameter p taking its values in a fixed interval \mathcal{Q} , we present a simple criterion of set inclusion which **guarantees that the Euler approximate solutions of Σ_{p_0} for some value $p_0 \in \mathcal{Q}$ converge to a limit cycle \mathcal{E}** . Moreover, we characterize a compact set \mathcal{I} containing \mathcal{E} which is invariant for the exact solutions of Σ_p whatever the value of $p \in \mathcal{Q}$. We illustrate the application of our method on the example of a parametric Van der Pol system driven by a periodic input.

Keywords: parametric differential equations, periodicity, uncertainty.

1. INTRODUCTION

Given a differential system $\Sigma : dx/dt = f(x)$ of dimension d , an initial point $x_0 \in \mathbb{R}^d$, a real $\varepsilon > 0$, and a ball $B_0 = \mathcal{B}(x_0, \varepsilon)$ ¹, we present here a simple method allowing to find a bounded invariant set of Σ containing the trajectories starting at B_0 . This invariant set has the form of a tube whose center at time t is the Euler approximate solution $\tilde{x}(t)$ of the system starting at x_0 , and radius is a function $\delta_\varepsilon(t)$ bounding the distance between $\tilde{x}(t)$ and an exact solution $x(t)$ starting at B_0 . The tube can thus be described as $\bigcup_{t \geq 0} B(t)$ where $B(t) \equiv \mathcal{B}(\tilde{x}(t), \delta_\varepsilon(t))$.

To find a *bounded* invariant, we then look for a positive real T such that $B((i+1)T) \subseteq B(iT)$ for some $i \in \mathbb{N}$. In case of success, the ball $B(iT)$ is guaranteed to contain the “stroboscopic” sequence $\{B(jT)\}_{j=i, i+1, \dots}$ of sets $B(t)$ at time $t = iT, (i+1)T, \dots$. It follows that the bounded portion $\bigcup_{t \in [iT, (i+1)T]} B(t)$ is equal to $\bigcup_{t \in [iT, \infty)} B(t)$, and thus constitutes the sought bounded invariant set.

We apply the finding of such a (forward) invariant set to the analysis of parameterized time-periodic differential systems. We illustrate our results on the example of a parametric Van der Pol system driven by a common periodic input.

1.0.0.1. Comparison with related work We explain here some similarities and differences of our method with several kinds of related work.

- There exists a trend of work on the generation of torus-shaped invariants using stroboscopic maps of quasi-periodic systems with possible parameters (see, e.g., Baresi and Scheeres (2016); Gómez and Mondelo (2001); Olikara and Scheeres (2012)). A first difference is that these works consider stroboscopic

mappings of *points* of \mathbb{R}^d , while our stroboscopic maps apply to *sets* of points. A second difference is that they often use a Fourier analysis in the *frequency domain* (using, e.g., the notion of “radii polynomials” Castelli and Lessard (2013)) while we remain in the *time domain*.

- Our method makes use of a rigorous time-integration method in order to enclose the exact solutions with tubes, which is similar to what is done using high order of Taylor method in ODE integration as proposed by Lohner or Taylor models Lohner (1987); Zgliczynski (2002). Such methods are used in Castelli and Lessard (2013); Kapela and Simo (2007) to rigorously compute the eigenvalues of a so-called “monodromy matrix”, which allows to determine the linear stability of the equilibrium points of the system. Unlike these works, our stability analysis does not try to compute such eigenvalues of monodromy matrices.
- Our method shares also some common features with the works of Aylward et al. (2008); Aminzare and Sontag (2014); van den Berg and Queirolo (2020), which aim at proving a *contractivity* property of the system (i.e., that any two solutions converge exponentially to each other). In Aminzare and Sontag (2014), contractivity amounts to the finding of a negative definite quadratic form (which is equivalent to the existence of a Lyapunov function for the system). In Aylward et al. (2008), “Squares-of-Sum programming is used to find ranges of uncertainty under which a system with uncertain perturbations is always contracting with the original contraction metric”. In van den Berg and Queirolo (2020), they turn the stability problem into the contractivity of a fixed point operator that is checked with the assistance of a computer. The difference here is that we do not try to prove a contractivity property, but only the existence of two set-valued snapshots, one of

¹ $\mathcal{B}(x_0, \varepsilon)$ is the set $\{z \in \mathbb{R}^d \mid \|z - x_0\| \leq \varepsilon\}$ where $\|\cdot\|$ denotes the Euclidean distance.

which is included in the other one. This is a much weaker property and easier to prove.

Our method is simple, efficient, and allows us to construct a **cyclic approximate solution** \mathcal{E} (using Euler's method) together with a (forward) invariant set \mathcal{I} around \mathcal{E} . Note however that, even if the approximate and exact solutions are very close in practice, **our method does not guarantee the formal existence of cyclic exact solutions inside \mathcal{I}** , which requires more technical methods such as Poincaré maps.

1.0.0.2. Plan of the paper In Section 2, we present our method, then explain how to apply it to the analysis of parameterized systems in Section 3. We conclude in Section 4.

2. METHOD

2.1 Euler's method and error bounds

Let us consider the differential system:

$$\frac{dx(t)}{dt} = f(x(t)),$$

with states $x(t) \in \mathbb{R}^d$. We will use $x(t; x_0)$ (or sometimes just $x(t)$) to denote the exact continuous solution of the system at time t , for a given initial condition x_0 . We use $\tilde{x}(t; y_0)$ (or just $\tilde{x}(t)$) to denote Euler's approximate value of $x(t; y_0)$ (defined by $\tilde{x}(t; y_0) = y_0 + tf(y_0)$ for $t \in [0, \tau]$, where τ is the integration time-step).

We suppose that we know a bounded region $\mathcal{S} \subset \mathbb{R}^d$ containing the solutions of the system for a set of initial conditions B_0 and a certain amount of time. We now give an upper bound to the error between the exact solution of the ODE and its Euler approximation on \mathcal{S} (see [Le Coënt and Fribourg \(2019\)](#); [Le Coënt et al. \(2017b\)](#)).

Definition 1. Let ε be a given positive constant. Let us define, for $t \in [0, \tau]$, $\delta_\varepsilon(t)$ as follows: if $\lambda < 0$:

$$\delta_\varepsilon(t) = \left(\varepsilon^2 e^{\lambda t} + \frac{C^2}{\lambda^2} \left(t^2 + \frac{2t}{\lambda} + \frac{2}{\lambda^2} (1 - e^{\lambda t}) \right) \right)^{\frac{1}{2}}$$

if $\lambda = 0$:

$$\delta_\varepsilon(t) = (\varepsilon^2 e^t + C^2(-t^2 - 2t + 2(e^t - 1)))^{\frac{1}{2}}$$

if $\lambda > 0$:

$$\delta_\varepsilon(t) = \left(\varepsilon^2 e^{3\lambda t} + \frac{C^2}{3\lambda^2} \left(-t^2 - \frac{2t}{3\lambda} + \frac{2}{9\lambda^2} (e^{3\lambda t} - 1) \right) \right)^{\frac{1}{2}}$$

where C and λ are real constants specific to function f , defined as follows:

$$C = \sup_{y \in \mathcal{S}} L \|f(y)\|,$$

where L denotes the Lipschitz constant for f , and λ is the “one-sided Lipschitz constant” (or “logarithmic Lipschitz constant” [Aminzare and Sontag \(2014\)](#)) associated to f , i. e., the minimal constant such that, for all $y_1, y_2 \in \mathcal{S}$:

$$\langle f(y_1) - f(y_2), y_1 - y_2 \rangle \leq \lambda \|y_1 - y_2\|^2, \quad (H0)$$

where $\langle \cdot, \cdot \rangle$ denotes the scalar product of two vectors of \mathcal{S} .

The constant λ can be computed using a nonlinear optimization solver (e. g., CPLEX [Cplex \(2009\)](#)) or using

the Jacobian matrix of f (see, e. g., [Aminzare and Sontag \(2014\)](#)).

Proposition 1. [Le Coënt et al. \(2017b\)](#) Consider the solution $x(t; y_0)$ of $\frac{dx}{dt} = f(x)$ with initial condition y_0 and the approximate Euler solution $\tilde{x}(t; x_0)$ with initial condition x_0 . For all $y_0 \in \mathcal{B}(x_0, \varepsilon)$, we have:

$$\|x(t; y_0) - \tilde{x}(t; x_0)\| \leq \delta_\varepsilon(t).$$

Proposition 1 underlies the principle of our set-based method where set of points are represented as balls centered around the Euler approximate values of the solutions. This illustrated in Fig. 1: for any initial condition x^0 belonging to the ball $\mathcal{B}(\tilde{x}^0, \delta(0))$ with $\delta(0) = \varepsilon$, the exact solution $x^1 \equiv x(\tau; x^0)$ belongs to the ball $\mathcal{B}(\tilde{x}^1, \delta_\varepsilon(\tau))$ where \tilde{x}^1 denotes the Euler approximation $\tilde{x}^0 + \tau f(\tilde{x}^0)$ at $t = \tau$.

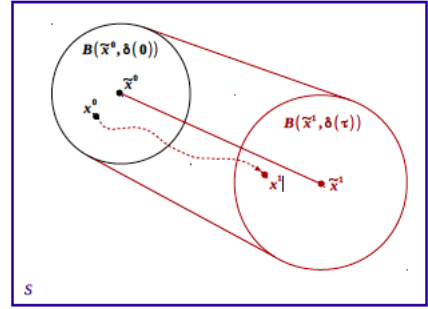


Figure 1. Illustration of Proposition 1

2.2 Systems with bounded uncertainty

Let us now show how the method extends to systems with “disturbance” or “bounded uncertainty”. A differential system with bounded uncertainty is of the form

$$\frac{dx(t)}{dt} = f(x(t), w(t)),$$

with $t \in \mathbb{R}_{\geq 0}^d$, states $x(t) \in \mathbb{R}^d$, and uncertainty $w(t) \in \mathcal{W} \subset \mathbb{R}^d$, where \mathcal{W} is a compact (i. e., closed and bounded) set. We assume that any possible disturbance trajectory is bounded at any point in time in the compact set \mathcal{W} . We denote this by $w(\cdot) \in \mathcal{W}$, which is a shorthand for $w(t) \in \mathcal{W}, \forall t \geq 0$. The diameter of \mathcal{W} (i. e., the maximal distance between two elements of \mathcal{W}) is denoted by $|\mathcal{W}|$. See [Schürmann and Althoff \(2017b,a\)](#) for details. We now suppose (see [Le Coënt et al. \(2017a\)](#)) that there exist constants $\lambda \in \mathbb{R}$ and $\gamma \in \mathbb{R}_{\geq 0}$ such that, for all $y_1, y_2 \in \mathcal{S}$ and $w_1, w_2 \in \mathcal{W}$:

$$\begin{aligned} & \langle f(y_1, w_1) - f(y_2, w_2), y_1 - y_2 \rangle \\ & \leq \lambda \|y_1 - y_2\|^2 + \gamma \|y_1 - y_2\| \|w_1 - w_2\| \quad (H1). \end{aligned}$$

This formula can be seen as a generalization of (H0) (see Section 2.1). Recall that λ has to be computed in the absence of uncertainty ($|\mathcal{W}| = 0$). The additional constant γ is used for taking into account the uncertainty w . Given λ , the constant γ can be computed itself using a nonlinear

optimization solver (e.g., CPLEX [Cplex \(2009\)](#)). Instead of computing them globally for \mathcal{S} , it is advantageous to compute λ and γ *locally* depending on the subregion of \mathcal{S} occupied by the system state during a considered interval of time. We now give a version of Proposition 1 with bounded uncertainty $w(\cdot) \in \mathcal{W}$, originally proved in [Le Coënt et al. \(2017a\)](#).

Proposition 2. *Le Coënt et al. (2017a) Consider a system Σ with bounded uncertainty of the form $\frac{dx(t)}{dt} = f(x(t), w(t))$ satisfying (H1).*

Consider a point $x_0 \in \mathcal{S}$ and a point $y_0 \in \mathcal{B}(x_0, \varepsilon)$. Let $x(t; y_0)$ be the exact solution of the system $\frac{dx(t)}{dt} = f(x(t), w(t))$ with bounded uncertainty \mathcal{W} and initial condition y_0 , and $\tilde{x}(t; x_0)$ the Euler approximate solution of the system $\frac{dx(t)}{dt} = f(x(t), 0)$ without uncertainty ($|\mathcal{W}| = 0$) with initial condition x_0 . We have, for all $w(\cdot) \in \mathcal{W}$ and $t \in [0, \tau]$:

$$\|x(t; y_0) - \tilde{x}(t; x_0)\| \leq \delta_{\varepsilon, \mathcal{W}}(t).$$

with

- if $\lambda < 0$,

$$\begin{aligned} \delta_{\varepsilon, \mathcal{W}}(t) = & \left(\frac{C^2}{-\lambda^4} (-\lambda^2 t^2 - 2\lambda t + 2e^{\lambda t} - 2) \right. \\ & + \frac{1}{\lambda^2} \left(\frac{C\gamma|\mathcal{W}|}{-\lambda} (-\lambda t + e^{\lambda t} - 1) \right. \\ & \left. \left. + \lambda \left(\frac{\gamma^2(|\mathcal{W}|/2)^2}{-\lambda} (e^{\lambda t} - 1) + \lambda \varepsilon^2 e^{\lambda t} \right) \right) \right)^{1/2} \quad (1) \end{aligned}$$

- if $\lambda > 0$,

$$\begin{aligned} \delta_{\varepsilon, \mathcal{W}}(t) = & \frac{1}{(3\lambda)^{3/2}} \left(\frac{C^2}{\lambda} (-9\lambda^2 t^2 - 6\lambda t + 2e^{3\lambda t} - 2) \right. \\ & + 3\lambda \left(\frac{C\gamma|\mathcal{W}|}{\lambda} (-3\lambda t + e^{3\lambda t} - 1) \right. \\ & \left. \left. + 3\lambda \left(\frac{\gamma^2(|\mathcal{W}|/2)^2}{\lambda} (e^{3\lambda t} - 1) + 3\lambda \varepsilon^2 e^{3\lambda t} \right) \right) \right)^{1/2} \quad (2) \end{aligned}$$

- if $\lambda = 0$,

$$\begin{aligned} \delta_{\varepsilon, \mathcal{W}}(t) = & (C^2 (-t^2 - 2t + 2e^t - 2) \\ & + (C\gamma|\mathcal{W}| (-t + e^t - 1) \\ & + (\gamma^2(|\mathcal{W}|/2)^2 (e^t - 1) + \varepsilon^2 e^t))^{1/2} \quad (3) \end{aligned}$$

We will sometimes write $\delta_{\mathcal{W}}(t)$ and $\delta(t)$ instead of $\delta_{\varepsilon, \mathcal{W}}(t)$ and $\delta_{\varepsilon}(t)$ respectively.

2.3 Correctness

Consider a differential system $\Sigma : dx/dt = f(x, w)$ with $w \in \mathcal{W}$, an initial point $x_0 \in \mathbb{R}^d$, a real $\varepsilon > 0$ and a ball $B_0 = \mathcal{B}(x_0, \varepsilon)$. Let $B_{\mathcal{W}}(t)$ denote $\mathcal{B}(\tilde{x}(t), \delta_{\varepsilon, \mathcal{W}}(t))$ where $\tilde{x}(t)$ is the Euler approximate solution of the system without uncertainty and initial condition x_0 ². It follows from Proposition 2 that $\bigcup_{t \geq 0} B_{\mathcal{W}}(t)$ is an invariant set containing B_0 . We can make an a stroboscopic map of this invariant. by considering periodically the set $B_{\mathcal{W}}(t)$ at the moments $t = 0, T, 2T$, etc., with $T = k\tau$ for some k (τ is the time-step used un Euler's method).

² Note that $B_{\mathcal{W}}(0) = B_0$ because $\tilde{x}(0) = x_0$ and $\delta_{\varepsilon, \mathcal{W}}(0) = \varepsilon$.

If moreover, we can find an integer $i \geq 0$ such that $B_{\mathcal{W}}((i+1)T) \subseteq B_{\mathcal{W}}(iT)$, then we have $B_{\mathcal{W}}(iT) = \bigcup_{j=i, i+1, \dots} B_{\mathcal{W}}(jT)$ and $\bigcup_{t \in [iT, (i+1)T]} B_{\mathcal{W}}(t) = \bigcup_{t \in [iT, \infty)} B_{\mathcal{W}}(t)$. The set $\bigcup_{t \in [iT, (i+1)T]} B_{\mathcal{W}}(t)$ is thus a *bounded invariant set* which contains all the solutions $x(t)$ starting at B_0 , for $t \in [iT, \infty)$. In the phase space, this invariant set has a “torus” shape. We have:

Proposition 3. *Suppose that there exist $T = k\tau$ with $k \in \mathbb{N}$, and $i \in \mathbb{N}$ such that:*

$$B_{\mathcal{W}}((i+1)T) \subseteq B_{\mathcal{W}}(iT).$$

Then $\mathcal{I}_{\mathcal{W}} \equiv \bigcup_{t \in [0, T]} B_{\mathcal{W}}(iT+t)$ is a compact (i.e., bounded and closed) invariant set containing, for $t \in [iT, \infty)$, all the solutions $x(t)$ of Σ with initial condition in B_0 .

3. APPLICATION TO PARAMETRIC SYSTEMS

Let us now consider a family $\{\Sigma_p\}_{p \in \mathcal{P}}$ of differential systems Σ_p of the form $dx/dt = f_p(x)$ involving a parameter $p \in \mathcal{P}$ (but no uncertainty). It is useful to find a subset \mathcal{Q} of \mathcal{P} and a system $\Sigma' : dx/dt = f(x, w)$ with uncertainty such that, for any $p \in \mathcal{Q}$, Σ_p is a particular form of Σ' for an appropriate uncertainty function $w(\cdot) \in \mathcal{W}$. This is useful to infer certain common properties of the solutions of $\{\Sigma_p\}_{p \in \mathcal{Q}}$ from the analysis of the system Σ' with uncertainty (cf. [Aylward et al. \(2008\)](#), Section 5).

Example 1. *Consider the Van der Pol system Σ_p with parameter $p \in \mathbb{R}$ driven by a periodic input of the form $0.015\cos(t)$ (see, e.g., [Capinski et al. \(arXiv:1905.08116, 2020\)](#)), with initial condition in $B_0 = \mathcal{B}(x_0, \varepsilon)$ for some given $x_0 \in \mathbb{R}^2$ and $\varepsilon > 0$ (see [van den Berg and Queirolo \(2020\)](#)):*

$$du_1/dt = u_2$$

$$du_2/dt = p(1 - u_1^2)u_2 - u_1 + 0.015\cos(t).$$

Consider now the system Σ' with uncertainty $w(\cdot) \in \mathcal{W} = [-0.1, 0.1]$ (hence $|\mathcal{W}| = 0.2$) and initial condition x_0 :

$$du_1/dt = u_2$$

$$du_2/dt = (p_0 + w(t))(1 - u_1^2)u_2 - u_1 + 0.015\cos(t),$$

with $p_0 = 0.4$. It is easy to see that each solution of Σ_p with $p \in \mathcal{Q} = [p_0 - 0.1, p_0 + 0.1] = [0.3, 0.5]$ is a particular solution of Σ' .

Theorem 1. *(cyclic approximate solution) Given a system $\Sigma' : dx/dt = f(x, w)$ with uncertainty $w \in \mathcal{W}$ and a set of initial conditions $B_0 \equiv \mathcal{B}(x_0, \varepsilon)$, suppose that any solution $x(t)$ of the parametric system $\Sigma_p : dx/dt = f_p(x)$ with $p \in \mathcal{Q} = [p_0 - |\mathcal{W}|/2, p_0 + |\mathcal{W}|/2]$ and initial condition x_0 is a solution of Σ' with initial set of conditions B_0 for some uncertainty function $w(\cdot) \in \mathcal{W}$. Let us suppose besides that, for Σ' , there exist $i \in \mathbb{N}$ and $T = k\tau$ with $k \in \mathbb{N}$ such that:*

$$B_{\mathcal{W}}((i+1)T) \subseteq B_{\mathcal{W}}(iT).$$

Then:

- (1) *When $n \rightarrow \infty$, the sequence $\{c_n \equiv \tilde{x}((i+n)T; x_0)\}$ converges to a limit $c^* \in \mathbb{R}^d$ satisfying $\tilde{x}(T; c^*) = c^*$.*
- (2) *The curve $\mathcal{E} \equiv \bigcup_{t \geq 0} \tilde{x}(t; c^*)$ is cyclic with period T , i.e.: $\tilde{x}(t+T; c^*) = \tilde{x}(t; c^*)$ for all $t \geq 0$.*
- (3) *When $t \rightarrow \infty$, $\tilde{x}(t; c_0)$ converges to \mathcal{E} . More precisely, for all $s \geq 0$, there exists $c_s^* \in \mathcal{E} : \|\tilde{x}(s+nT; c_0) - c_s^*\| \rightarrow 0$ as $n \rightarrow \infty$. This means that \mathcal{E} is an*

attractive limit cycle for the approximate solution $\tilde{x}(t; c_0)$ (whence $\tilde{x}(t; x_0)$) as $t \rightarrow \infty$.

- (4) The set $\mathcal{I}_0 = \bigcup_{t \geq 0} \mathcal{B}(\tilde{x}(t; c_0), \delta(iT + t))$ includes \mathcal{E} and is (forward) invariant for Σ_{p_0} , i.e.: all solution of Σ_{p_0} starting from \mathcal{I}_0 remains in \mathcal{I}_0 .
- (5) For each $p \in \mathcal{Q}$, the set $\mathcal{I}_W = \bigcup_{t \in [0, T]} B_W(iT + t)$ is (forward) invariant for Σ_p , i.e.: all solution of Σ_p starting from \mathcal{I}_W remains in \mathcal{I}_W .

Proof. (sketch) The arguments of the 5 items of the theorem are as follows:

- (1) As the balls $B_W(i + nT)$ are included in each other, this implies that their radii ε_n are decreasing and converge to a limit ε^* . This also implies that the centers c_n of these balls converge to a point $c^* \in \mathbb{R}^d$, and that balls $B_W(i + nT)$ converge to the ball $\mathcal{B}(c^*, \varepsilon^*)$. This limit ball is a fixed point of the function mapping a ball $\mathcal{B}(c, \rho)$ to $\mathcal{B}(\tilde{x}(T; c), \delta_{\rho, W}(T))$, and satisfies: $\mathcal{B}(\tilde{x}(T; c^*), \delta_{\varepsilon^*, W}(T)) = \mathcal{B}(c^*, \varepsilon^*)$. In particular, we have: $\tilde{x}(T; c^*) = c^*$.
- (2) Follows from $\tilde{x}(T; c^*) = c^*$ (see above) and $\tilde{x}(t + T; c^*) = \tilde{x}(t; \tilde{x}(T, c^*)) = \tilde{x}(t; c^*)$.
- (3) For all $s \in [0, T)$, $\tilde{x}(s + nT; c_0) = \tilde{x}(s; \tilde{x}(nT, c_0)) = \tilde{x}(s; c_n)$. It follows, that for all $s \in [0, T)$, $\|\tilde{x}(s + nT; c_0) - c_s^*\| = \|\tilde{x}(s; c_n) - c_s^*\| \rightarrow 0$ as $n \rightarrow \infty$ with $c_s^* \equiv \tilde{x}(s; c^*)$ (thanks to the continuity of $\tilde{x}(s; c)$ w.r.t. c).
- (4) Follows from Proposition 1.
- (5) Follows from Proposition 3.

□

Remark 1. Theorem 1 states the existence of an approximate cyclic solution \mathcal{E} of Σ_{p_0} ; in practice, when the integration time-step τ is sufficiently small, \mathcal{E} is very close to the cyclic exact solution if such a cycle exists. But Theorem 1 does not guarantee by itself the existence of an exact cyclic solution. Although we know that certain exact solutions of Σ_{p_0} lie in \mathcal{I}_0 close to \mathcal{E} , we do not know a priori if some of them are cyclic. To prove formally the existence of an exact cyclic solution, one could have to resort to specific notions of contractivity (see, e.g. [Manchester and Slotine \(2013\)](#); [Aminzare and Sontag \(2014\)](#); [Capinski et al. \(arXiv:1905.08116, 2020\)](#)).³

The implementation has been done in Python and corresponds to a program of around 500 lines. The source code is available at lipn.univ-paris13.fr/~jerray/parameter/. In the experiments below, the program runs on a 2.80 GHz Intel Core i7-4810MQ CPU with 8 GiB of memory. Given $x_0, \tau, \varepsilon, |W|$, the program searches heuristically for values of $i \in \mathbb{N}$ and $T = k\tau$ (for some $k \in \mathbb{N}$) in order to verify $B_W((i + 1)T) \subseteq B_W(iT)$. This is illustrated in the following example.

Example 2. Consider the system Σ_p of Example 1 and the system Σ' with uncertainty $|W| = 0.2$, and let $p_0 = 0.4$. Consider the set of initial conditions $\mathcal{B}(x_0, \varepsilon)$ with $x_0 = (1.46898897, -1.12538766)$ and $\varepsilon = 0.1$. For $T = 6.368 = k\tau$ with $\tau = 10^{-3}$, we find:

$$\tilde{x}(0) = (1.46898897, -1.12538766), \delta_W(0) = 0.1$$

³ In dimension $d = 2$, the existence of such a cycle is guaranteed by the Bendixon-Poincaré theorem.

$$\tilde{x}(T) = (1.45389133, -1.10970492),$$

$$\delta_W(T) = 2.437975771955677$$

$$\tilde{x}(2T) = (1.45195751, -1.11004367),$$

$$\delta_W(2T) = 2.637252198149563$$

$$\tilde{x}(3T) = (1.45230073, -1.11065593),$$

$$\delta_W(5T) = 2.652749677582014$$

$$(\dots)$$

$$\tilde{x}(13T) = (1.49176459, -1.09165581),$$

$$\delta_W(13T) = 2.645700321656063$$

$$\tilde{x}(14T) = (1.49470193, -1.09069935),$$

$$\delta_W(14T) = 2.644674179178997$$

$$\tilde{x}(15T) = (1.49666192, -1.09054882),$$

$$\delta_W(15T) = 2.642640758083935$$

$$\tilde{x}(16T) = (1.49747851, -1.09133825),$$

$$\delta_W(16T) = 2.6411743966251087$$

$$\tilde{x}(17T) = (1.49699953, -1.09318874),$$

$$\delta_W(17T) = 2.631805337566251$$

$$\tilde{x}(18T) = (1.49508659, -1.09620741),$$

$$\delta_W(18T) = 2.6266533499722065$$

$$\tilde{x}(19T) = (1.49161476, -1.10048667),$$

$$\delta_W(19T) = 2.621622599187829$$

$$\tilde{x}(20T) = (1.48647167, -1.10610402),$$

$$\delta_W(20T) = 2.614143707597656.$$

We have: $B_W((i + 1)T) \subset B_W(iT)$ for $i = 14$. The computation took 1120s of CPU time. This shows that the invariant \mathcal{I}_W has a torus shape for $t \in [14T, 15T]$, and contains the solutions of Σ_p for each $p \in [p_0 - |W|/2, p_0 + |W|/2]$. Fig. 2 shows the cyclic approximate solution \mathcal{E} of Σ_{p_0} in the plane phase (top), and the radius $\delta(t)$ of the invariant \mathcal{I}_0 of Σ_{p_0} (bottom). As $\delta(t)$ becomes rapidly neglectible, the exact solutions of Σ_{p_0} and \mathcal{E} practically coincide within \mathcal{I}_0 .

The invariant \mathcal{I}_W with $|W| = 0.2$ is depicted in green on Fig. 3, and it can be seen that \mathcal{I}_W encloses all the solutions of Σ_p for $p = p_0, p_0 \pm |W|/2$ (represented in red, cyan and blue) for $t \in [15T, 20T]$, as stated by Proposition 2.

4. CONCLUSION

Given a parametric differential system parameter Σ_p (with a parameter p taking its values in an interval of the form $\mathcal{Q} = [p_0 - |W|/2, p_0 + |W|/2]$), we have introduced a simple condition of inclusion of sets (Euclidean balls) which guarantees that the approximate Euler solutions of Σ_{p_0} are attracted by a limit cycle \mathcal{E} , which is itself a cyclic approximate solution of Σ_{p_0} . Moreover, we have introduced a toric set \mathcal{I}_0 around \mathcal{E} which is invariant for Σ_{p_0} , and whose radius $\delta(t)$ becomes in practice quickly very small. This shows that the exact solutions of Σ_{p_0}

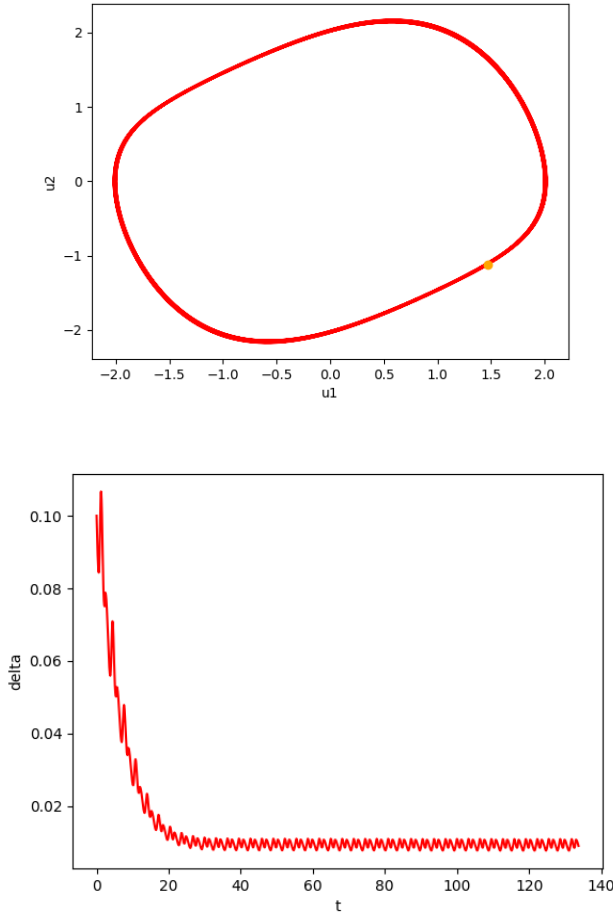


Figure 2. Top: the approximate Euler solution of Σ_{p_0} ($p_0 = 0.4$) in the phase plan near the limit cycle \mathcal{E} . Bottom: the error bound $\delta(t)$ for $t \in [0, 20T]$ when $|\mathcal{W}| = 0$. The invariant \mathcal{I}_0 is a torus centered around \mathcal{E} (top), and its radius $\delta(t)$ becomes rapidly neglectible (bottom). This shows that the approximate and exact solutions of Σ_{p_0} are rapidly almost identical.

exist in the close neighborhood of the cycle \mathcal{E} and have themselves an almost cyclic behavior. Finally, we have constructed a compact set $\Sigma_{\mathcal{W}}$ centered also on \mathcal{E} , whose radius $\delta_{\mathcal{W}}(t)$ is now non negligible, which is invariant for every system Σ_p ($p \in \mathcal{Q}$). We hope that this method, illustrated on the example of a parametric Van der Pol system, opens an alternative practical way to the complex techniques based on contractivity, Lyapunov functions or Poincare maps that are used presently to **show the existence of attractive limit cycles**.

REFERENCES

- Aminzare, Z. and Sontag, E.D. (2014). Contraction methods for nonlinear systems: A brief introduction and some open problems. In *53rd IEEE Conference on Decision and Control, CDC 2014, Los Angeles, CA, USA, December 15-17, 2014*, 3835–3847.
- Aylward, E.M., Parrilo, P.A., and Slotine, J.E. (2008). Stability and robustness analysis of nonlinear systems via contraction metrics and SOS programming. *Automatica*, 44(8), 2163–2170. doi:

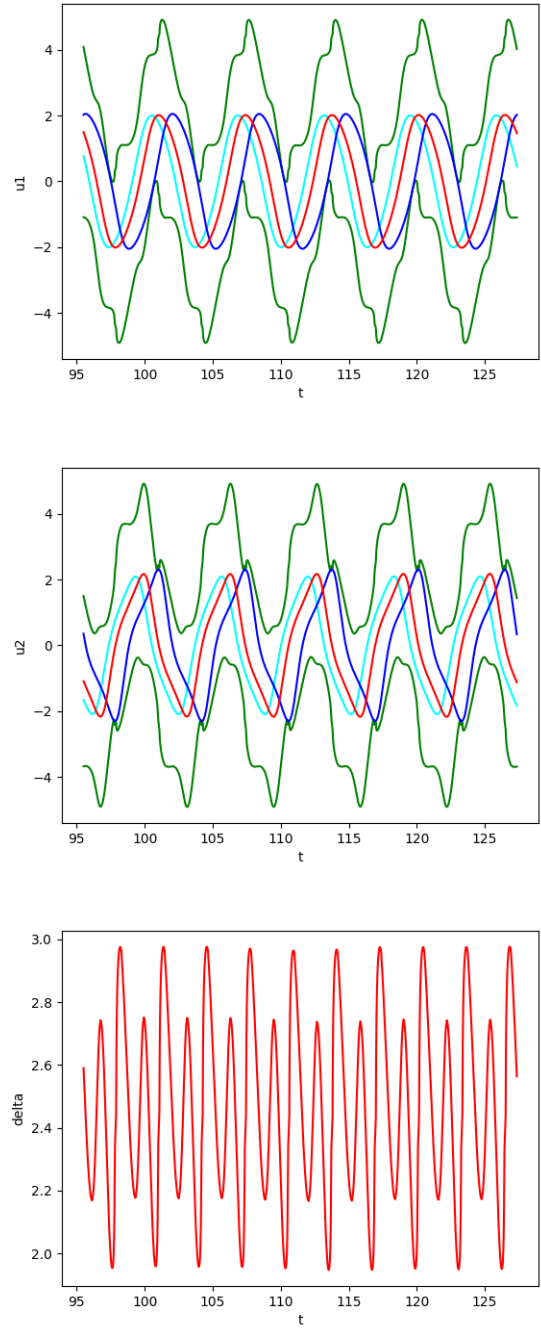


Figure 3. The top and middle figures represent $u_1(t)$ and $u_2(t)$ for $t \in [15T, 20T]$: the red, cyan and blue oscillatory curves correspond to $\Sigma_{p_0}, \Sigma_{p_0-|\mathcal{W}|/2}, \Sigma_{p_0+|\mathcal{W}|/2}$ respectively with $p_0 = 0.4$ and $|\mathcal{W}| = 0.2$; the parallel green curves delimit the invariant torus $\mathcal{I}_{\mathcal{W}}$ which is centered around the (red) solution of Σ_{p_0} , with a radius $\delta_{\mathcal{W}}(t)$ that is represented in the lower figure. On checks on the top and middle figures that $\mathcal{I}_{\mathcal{W}}$ encloses the solutions of Σ_p for $p = p_0, p_0 \pm |\mathcal{W}|/2$.

10.1016/j.automatica.2007.12.012. URL <https://doi.org/10.1016/j.automatica.2007.12.012>.

Baresi and Scheeres (2016). Quasi-periodic invariant tori of time-periodic dynamical systems: Applications

- to small body exploration. In *67th International Conference on Astronautical Congress, Guadalajara, Mexico*.
- Capinski, M.J., Fleurantin, E., and James, J.D.M. (arXiv:1905.08116, 2020). Computer assisted proofs of attracting invariant tori for ODEs.
- Castelli, R. and Lessard, J.P. (2013). Rigorous numerics in Floquet theory: computing stable and unstable bundles of periodic orbits. *SIAM Journal on Applied Dynamical Systems*, 12(1), 204–245.
- Cplex, I.I. (2009). V12. 1: User’s manual for cplex. *International Business Machines Corporation*, 46(53), 157.
- Gómez, G. and Mondelo, J.M. (2001). The dynamics around the collinear equilibrium points of the RTBP. *Physica D: Nonlinear Phenomena*, 157(4), 283–321.
- Kapela, T. and Simo, C. (2007). Computer assisted proofs for nonsymmetric planar choreographies and for stability of the eight. *Nonlinearity*, 20(5).
- Le Coënt, A., Alexandre Dit Sandretto, J., Chapoutot, A., Fribourg, L., De Vuyst, F., and Chamoin, L. (2017a). Distributed control synthesis using Euler’s method. In *Proc. of International Workshop on Reachability Problems (RP’17)*, volume 247 of *Lecture Notes in Computer Science*, 118–131. Springer.
- Le Coënt, A., De Vuyst, F., Chamoin, L., and Fribourg, L. (2017b). Control synthesis of nonlinear sampled switched systems using Euler’s method. In *Proc. of International Workshop on Symbolic and Numerical Methods for Reachability Analysis (SNR’17)*, volume 247 of *EPTCS*, 18–33. Open Publishing Association.
- Le Coënt, A. and Fribourg, L. (2019). Guaranteed optimal reachability control of reaction-diffusion equations using one-sided Lipschitz constants and model reduction. In *Model-Based Design of Cyber Physical Systems (CyPhy’19)*, N.-Y., USA.
- Lohner, R.J. (1987). Enclosing the solutions of ordinary initial and boundary value problems. *Computer Arithmetic*, 255–286.
- Manchester, I.R. and Slotine, J.E. (2013). Transverse contraction criteria for existence, stability, and robustness of a limit cycle. In *Proceedings of the 52nd IEEE Conference on Decision and Control, CDC 2013, December 10-13, 2013, Firenze, Italy*, 5909–5914. IEEE. doi:10.1109/CDC.2013.6760821. URL <https://doi.org/10.1109/CDC.2013.6760821>.
- Olikara, Z.P. and Scheeres, D.J. (2012). Numerical method for computing quasi-periodic orbits and their stability in the restricted three-body problem. *Advances in the Astronautical Sciences*, 145.
- Schürmann, B. and Althoff, M. (2017a). Guaranteeing constraints of disturbed nonlinear systems using set-based optimal control in generator space. *IFAC-PapersOnLine*, 50(1), 11515 – 11522. doi: <https://doi.org/10.1016/j.ifacol.2017.08.1617>. URL <http://www.sciencedirect.com/science/article/pii/S2405896317322152>. 20th IFAC World Congress.
- Schürmann, B. and Althoff, M. (2017b). Optimal control of sets of solutions to formally guarantee constraints of disturbed linear systems. In *2017 American Control Conference, ACC 2017, Seattle, WA, USA, May 24-26, 2017*, 2522–2529. doi:10.23919/ACC.2017.7963332.
- van den Berg, J.B. and Queirolo, E. (2020). A general framework for validated continuation of periodic orbits in systems of polynomial ODEs. *Journal of Computational Dynamics*, 0(2158-2491-2019-0-10). doi: 10.3934/jcd.2021004.
- Zgliczynski, P. (2002). C1 Lohner algorithm. *Found. Comput. Math.*, 2(4).